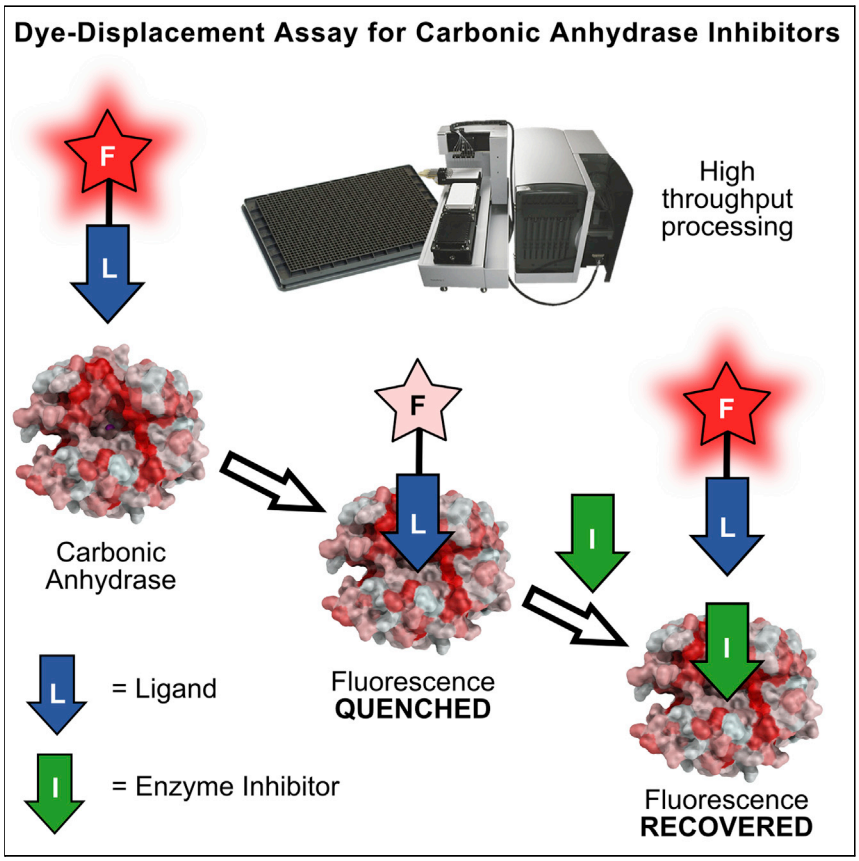
Chem

CellPress

Article

Fluorescence-Based Assay for Carbonic Anhydrase Inhibitors



Anzenbacher, Jr. and coworkers describe a fluorescence-based assay that can evaluate the efficacy of potential carbonic anhydrase II (CA II) inhibitors. This high-throughput assay utilizes an indicator-displacement assay concept based on treating a fluorescent indicator with the enzyme to quench the indicator bound inside the enzyme-binding pocket. The fluorescence recovery is directly proportional to the affinity of the inhibitor for the enzyme, which enables evaluation of the carbonic anhydrase inhibitor as a potential drug.

Petr Koutnik, Elena G. Shcherbakova, Samer Gozem, Mehmet G. Caglayan, Tsuyoshi Minami, Pavel Anzenbacher, Jr.

pavel@bgsu.edu

HIGHLIGHTS

Fluorescence-based assay for carbonic anhydrase inhibitors is presented

Present assay enables evaluation of potential inhibitor drugs for carbonic anhydrase

This assay is amenable to high-throughput screening of potential inhibitor drugs

Koutnik et al., Chem 2, 271–282
February 9, 2017 © 2017 Elsevier Inc.
http://dx.doi.org/10.1016/j.chempr.2017.01.011

Chem

CellPress

Article

Fluorescence-Based Assay for Carbonic Anhydrase Inhibitors

Petr Koutnik,[1] Elena G. Shcherbakova,[1] Samer Gozem,[2] Mehmet G. Caglayan,[1] Tsuyoshi Minami,[1] and Pavel Anzenbacher, Jr.[1,3,*]

SUMMARY

Carbonic anhydrases are implicated in a number of diseases, including glaucoma, cancer, epilepsy, and others. Here, we present a fluorescence-based assay that utilizes the indicator-displacement assay concept and can be used to prescreen inhibitor candidates to treat such conditions. We designed and synthesized fluorescent indicators that bind carbonic anhydrase and display fluorescence quenching in the presence of the enzyme. Their fluorescence is, however, recovered when a competitive inhibitor is added. To investigate the utility of this dye-displacement system and its potential for use in high-throughput screening, we designed a fluorescence microarray. This confirmed the potential of the approach for both qualitative and quantitative analysis. Using AutoDock Vina and AutoDock4$_{Zn}$, we compared the results of the assay with ligand docking calculations. We show that the dye-displacement arrays are more accurate and sensitive than docking calculations and that these two tools can be used together to efficiently screen libraries of potential carbonic anhydrase inhibitors in a high-throughput manner.

INTRODUCTION

Carbonic anhydrases (CAs; EC 4.2.1.1) are ubiquitous Zn^{2+} metalloenzymes.[1–3] The 15 known human CA isozymes display different catalytic efficiency, subcellular localization, and tissue distribution.[4–6] However, all CAs catalyze the reversible hydration of carbon dioxide to bicarbonate ($CO_2 + H_2O \leftrightarrows HCO_3^- + H^+$).[7–9] Many of the CA isozymes involved in these processes are important therapeutic targets in the treatment of a range of disorders, including edema,[10,11] glaucoma,[12,13] obesity,[14,15] cancer,[16,17] epilepsy,[18,19] altitude sickness,[20,21] and osteoporosis.[22,23] Because of the importance of this family of proteins, numerous studies have been devoted to the design of isozyme-specific CA inhibitors, displaying few side effects.[24,25] Among CA inhibitors, the most promising class are unsubstituted sulfonamides.[26–28] Current approaches to estimating inhibitor efficiency have for the most part been limited to molecular docking calculations[29–31] or measurement of catalytic activity.[32,33] Fluorescence-based assays, despite their potential, are still less frequent.[34,35] However, molecular docking is often not quantitative, and measuring catalytic activity is difficult in a high-throughput fashion to screen large libraries of ligands. We decided to use a supramolecular chemistry approach based on an indicator-displacement assay[36] in order to bridge the gap between the inexpensive but simplified docking models and the accurate but delicate catalytic activity studies.

In order to design a suitable indicator, we exploited the affinity of sulfonamides for the Zn^{2+} catalytic site of CAs. The sulfonamide ligand is attached to a fluorescent dye

The Bigger Picture

Carbonic anhydrase inhibitors are important for the treatment of various ailments. For the development of new drugs, large libraries of potential inhibitors must be screened in catalytic experiments. These inhibitors are not easily amenable to high-throughput screening or computational (docking) analyses. The fluorescence-based method presented in this work utilizes an indicator-displacement assay, a concept known in supramolecular chemistry, to provide quantitative insight into the binding of carbonic anhydrase inhibitors. The results of the assay are compared with ligand docking calculations. We show that the dye-displacement assay is more accurate and sensitive than docking calculations. The present method requires only standard fluorescence formats and tools, which makes the assay easy to adopt and uniquely suited for high-throughput screening. Similar methodologies could be used in the future to develop inhibitors for other enzymes and proteins.

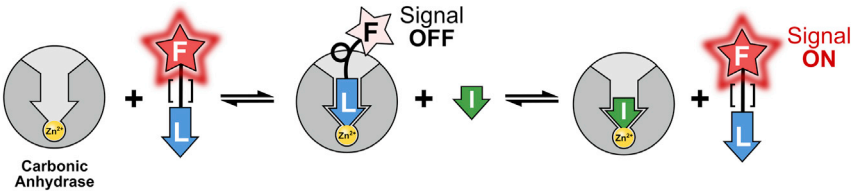


Figure 1. Design of the Indicator-Displacement Fluorescence-Based Assay for Carbonic Anhydrase

Fluorescent indicator comprising a specific high-affinity moiety (L) and a fluorophore (F) is bound by the enzyme, a process associated with attenuated fluorescence. Replacement of the indicator by the inhibitor (I) causes fluorescence recovery.

whose function is to signal the binding event.[37,38] Such an indicator is bound by the CA with an associated change in indicator fluorescence. In the presence of a CA-binding inhibitor, the indicator is displaced from the enzyme, causing the original fluorescence to be re-established as shown in the scheme in Figure 1. We believe that this principle is general and could be used whenever an enzyme binds a known ligand that can be conjugated to a dye.

RESULTS AND DISCUSSION

Indicator Design and Synthesis

Detailed synthetic routes for indicators **S1**–**S5** (shown in Figure 2) are summarized in the Supplemental Information (see Supplemental Experimental Procedures and Schemes S2.1–S2.6) together with information on their photophysical properties. All of the indicators prepared feature the 1,3,4-thiadiazol-5-yl-2-sulfonamide moiety, known to possess a high binding affinity toward the zinc ion embedded in the binding pocket of CAs.[2] This high-affinity moiety was conjugated with three different fluorophores: 7-methoxycoumarin (**S1** and **S2**), (dimethylamino)naphthalene (**S3** and **S4**), and pyrene (**S5**). One type of indicator was prepared by coupling of the 1,3,4-thiadiazol-5-yl-2-sulfonamide moiety directly with fluorophore (**S1** and **S3**), whereas the other type includes a six- or nine-atom-long spacer linking the ligand with the fluorophore (**S2**, **S4**, and **S5**). Interestingly, the fluorescence quantum yields (see Table S2 and Figure S3) show that higher values were obtained for extended indicators **S2**, **S4**, and **S5** (52%, 10%, and 28%, respectively) than for their short congeners **S1** and **S3** (17% and 1%, respectively).

Fluorescence Titrations

To confirm that the indicators interact with CA, we carried out fluorescence titrations. Indicator **S1** (Figure 3A) showed fluorescence signal quenching by 90% upon the addition of an incremental amount of carbonic anhydrase isozyme II (bCA II). 7-Alcoxycoumarins (**S1** and **S2**) are known to exhibit a solvent-dependent fluorescence such that the fluorescent intensity increases with increasing polarity of the medium (e.g., the fluorescence quantum yield of 7-methoxycoumarin is 0.5 in buffer but only 0.03 in methanol).[39] This is different from the environment-sensitive fluorophores (**S3**–**S5**), where fluorescence amplification is observed[40–42] before addition of the CA inhibitor.[37]

We also carried out fluorescence titration experiments with isozyme II of human carbonic anhydrase (hCA II) to see how the fluorescence response differs between the two isozymes (see Figures S4–S17). It is known that the sequence homology between bCA II and hCA II is about 80%.[43] Not surprisingly, hCA II provides a comparable response with only a slightly higher binding constant (Table 1). To prove that the response is specifically related to CAs, we performed the same experiment with

[1]Department of Chemistry, Bowling Green State University, Bowling Green, OH 43403, USA

[2]Department of Chemistry, University of Southern California, Los Angeles, CA 90089, USA

[3]Lead Contact

*Correspondence: pavel@bgsu.edu

http://dx.doi.org/10.1016/j.chempr.2017.01.011

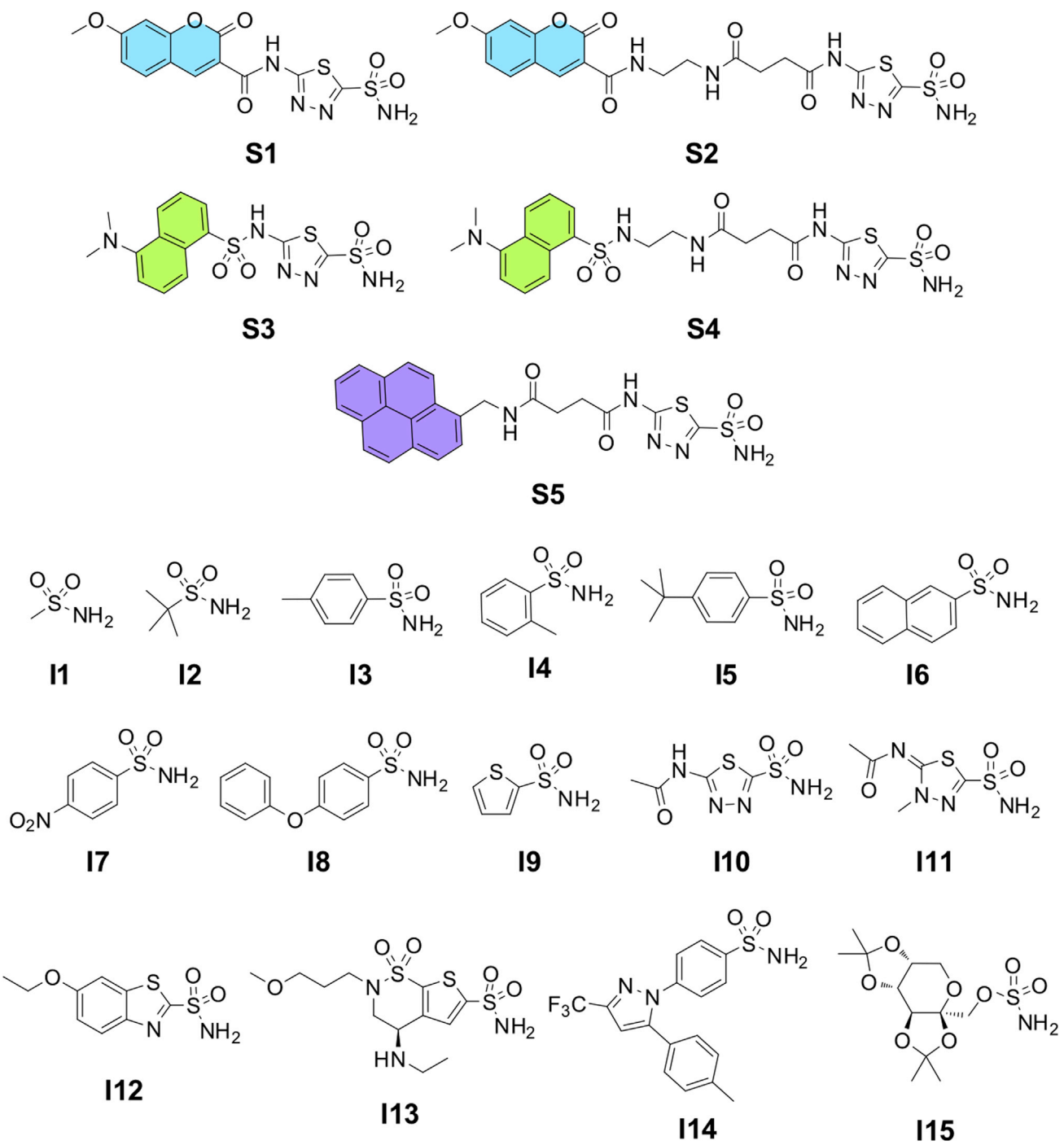


Figure 2. Fluorescent High-Affinity Sulfonamide Indicators and Inhibitors of Carbonic Anhydrases Used in This Study

S1–S5 are shown at the top, and **I1–I15** are shown at the bottom: **I1**, methanesulfonamide; **I2**, *tert*-butylsulfonamide; **I3**, *p*-methylbenzene sulfonamide; **I4**, *o*-methylbenzene sulfonamide; **I5**, 4-*tert*-butylbenzene sulfonamide; **I6**, naphthalene 2-sulfonamide; **I7**, *p*-nitrobenzene sulfonamide; **I8**, *p*-phenoxybenzene sulfonamide; **I9**, 2-thiophene sulfonamide; **I10**, acetazolamide; **I11**, methazolamide; **I12**, ethoxzolamide; **I13**, brinzolamide; **I14**, celecoxib; and **I15**, topiramate.

human serum albumin (hSA)[44] and found a negligible response of indicator **S1** on addition of hSA (Figure 3B). Table 1 summarizes the binding constants for indicators **S1–S5** obtained from fluorescence titration experiments for hCA II and bCA II.

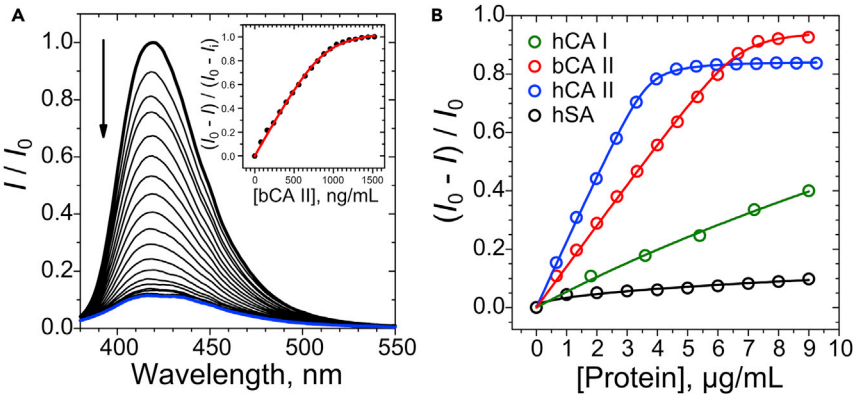


Figure 3. A Direct Fluorescence Titration of the Fluorescent Probe with bCA II

(A) Fluorescence titration of **S1** (500 nM) upon the addition of an incremental amount of bCA II in aqueous HEPES solution (50 mM and pH 7.2) with fluorescence isotherm (inset). λ_{EXC} = 373 nm and [bCA II] = 0–1520 ng/mL.

(B) Fluorescence titration isotherms of **S1** (5 µM) upon the addition of incremental amounts of bovine and human carbonic anhydrase isozyme I and II and human serum albumin (bCA II, hCA I, hCA II, and hSA, respectively) in aqueous HEPES buffer (50 mM and pH 7.2). λ_{EXC} = 373 nm.

The affinity constants obtained show that the length of the linker chain dramatically affects the binding affinity toward the target enzyme. A lower affinity and smaller magnitude of difference between the on and off states was recorded for indicators with longer linkers. This suggests that the distance between the fluorescent dye and the binding site might be too large to significantly affect the photophysical properties of the reporter. On the other hand, the effect of the short linker affects the response of the indicator more dramatically, most likely because the indicator is more efficiently accommodated within the binding pocket. This is supported by the docking calculations performed with AutoDock4$_{Zn}$[45] (for details, see Figures S53 and S54). Figures 4A and 4C show the binding of indicators **S1** and **S2** to the Zn^{2+} center of the hCA II and their interaction with the solvent-accessible surface, rendered by hydrophobicity mapping. The hydrophobic region is shown in red. Figure 4C shows the indicator **S2** with the loop of the spacer protruding out of the binding pocket. Figures 4B and 4D show the indicators **S1** and **S2** bound to hCA II and their interaction with participating amino acid residues. Coumarin in **S1** is included within the binding cavity, where it interacts with the hydrophobic domain, but in **S2** the long flexible spacer forces the coumarin to stick out of the binding pocket of the enzyme, where it encounters the solvent molecules. This most likely results in a smaller effect on the magnitude of the change in fluorescence intensity between the free and bound states of the indicator.

Displacement Assay

As a result of the large changes in fluorescence between free and bound indicator, it is possible to exploit this sensitivity by setting up an indicator-displacement assay (Figure 1). Figure 3 shows the quenching of the indicator upon the addition of bCA II, and Figure 5 shows the recovery of the fluorescence on addition of a CA inhibitor. To further investigate the ability of the CA-indicator complexes to signal the presence and affinity of CA inhibitors, we used a library of non-fluorescent sulfonamide CA inhibitors to set up a competitive assay (Figure 2, bottom). The structures were selected so that various electronic and steric effects on the competitive binding could be evaluated. The library included two aliphatic (**I1**, **I2**) and six aromatic (**I3**–**I9**) sulfonamides as well as five drugs of clinical relevance: acetazolamide (**I10**),

Table 1. Binding Affinities K_S of Indicators S1–S5 to Human and Bovine Carbonic Anhydrase II as Obtained from Fluorescence Titration and Molecular Docking Calculations

Indicator[a]	Binding Affinity K_S (M^{-1})[b]			
	Human CA II		Bovine CA II	
	Experiment	Docking[c]	Experiment	Docking[c]
S1	6.5×10^8	1.2×10^6	5.8×10^8	2.3×10^5
S2	5.0×10^7	2.3×10^5	9.8×10^7	4.4×10^5
S3	1.3×10^8	3.7×10^5	1.8×10^8	2.7×10^5
S4	4.9×10^7	1.4×10^5	2.0×10^8	1.4×10^6
S5	$>10^6$	7.8×10^6	1.9×10^7	6.2×10^5

[a]500 nM.
[b]In aqueous HEPES buffer (50 mM and pH 7.2).
[c]Ligand docking calculations using AutoDock Vina.

methazolamide (**I11**), ethoxzolamide (**I12**), brinzolamide (**I13**), and celecoxib (**I14**). To illustrate the utility of the assay, we also included an isosteric sulfamate inhibitor topiramate (**I15**). In order to determine the affinity constants of the model inhibitors **I1**–**I15** to carbonic anhydrase, we carried out fluorescence titrations and calculated binding affinities from the titration isotherms (see Equations S1–S9 for details).

Docking Analysis and Comparison with Experimental Data

The above results obtained from the displacement assay were then compared with the results derived from docking calculations using AutoDock Vina[46] (details of the calculations are described in the Supplemental Information, "Molecular Modeling: Sensors and Inhibitors Docking Study"). We used **S1** for the fluorescence titrations because this indicator provided a relatively high quantum yield and a strong response. A solution of indicator **S1** was premixed with bCA II at a concentration corresponding to the saturation region of the fluorescence isotherm (9.6 μg/mL), and the resulting mixture was titrated with the inhibitor solution (Figure 4). Table 2 summarizes the binding affinities obtained from competitive titration experiments for inhibitors **I1**–**I14** and the values calculated by AutoDock Vina (see Figures S19–S31 and Tables S5, S18, and S19 for details).

In the case of inhibitors **I1** and **I2**, no change in fluorescence intensity was observed (up to 1 mM), presumably because the binding affinity of the thiadiazole sulfonamide-based indicator **S1** to bCA II is several orders of magnitude higher than those of inhibitors **I1** and **I2**. An interesting trend, however, was observed for aromatic and heteroaromatic inhibitors **I3**–**I9**. *p*-Substituted benzene sulfonamides **I3** and **I5** display higher binding constants than *o*-methylbenzene sulfonamide **I4** as a result of the steric hindrance of the methyl group near the sulfonamide group that binds to zinc at the active site of the protein. The constant obtained for **I5** was higher than that for **I3**. Similarly, the hydrophobic residues in **I6** and **I8** resulted in higher affinity. This is rationalized by the observation that two or three hydrophobic rings provide high affinity, a structural feature displayed in a number of CA inhibitor-based drugs such as ethoxzolamide **I12**, brinzolamide **I13**, and celecoxib **I14**. 4-Nitrobenzene sulfonamide **I7** lacks an extended aromatic system or low-polarity substituents; we believe that its surprising affinity to CA is a result of increased acidity and metal-coordinating ability of the sulfonamide group, imparted by the $-NO_2$ substituent. Thiophene sulfonamide **I9** showed low affinity to CA, as reflected by both the assay and the calculation. As expected, the highest apparent constant was observed for inhibitors **I12** and **I13**, of which **I13** was the highest. The experimentally determined affinity constants ranged from 10^4 to 10^{11} M^{-1} (Table 2). Docking calculations also

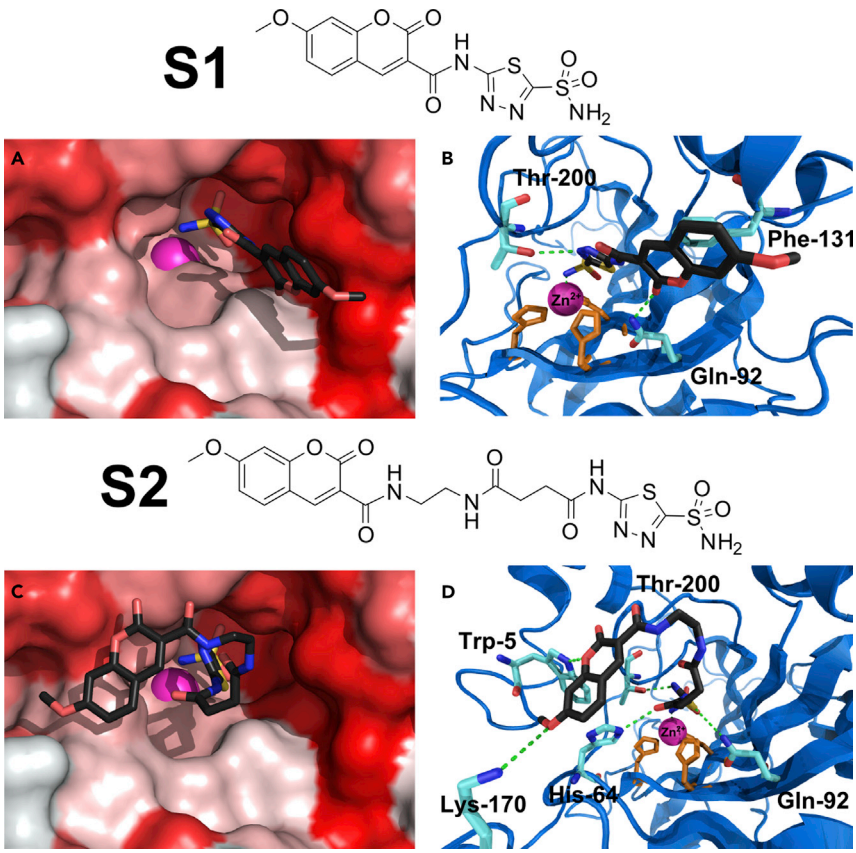


Figure 4. Indicators Docking

(A) Surface hydrophobicity mapping of the molecular surface of human CA II shows hydrophobic (red) areas with a binding pocket in the center.

(B) **S1** is tightly bound in the pocket while strongly interacting with the hydrophobic patch on the surface.

(C) The fluorophore in **S2** is only weakly interacting with the CA II binding pocket, as shown in the surface hydrophobicity mapping.

(D) The analysis of amino acid residues interacting with the long-spacer indicator **S2** suggests weak binding.

indicated that **I10**–**I14** were among the high-affinity ligands; the highest computed constant was for *p*-phenoxybenzene sulfonamide **I8** (2.8×10^6 M^{-1}).

Perhaps the most important outcome of this study is the observation that the magnitude of the indicator fluorescence response observed upon addition of inhibitor directly correlates with the affinity of the inhibitor for CA. Following the data in Figure 6, one can see that, for example, at inhibitor concentrations of 5–20 μM, the order of the observed fluorescence response is **I10** > **I11** > **I8** > **I7** > **I14** > **I6** > **I5** ≫ **I9**. **I12** (ethoxzolamide) and **I13** (brinzolamide) display a significantly higher response and affinity toward CAs. Thus, any unknown inhibitor candidate displaying a fluorescence response amplification between **I12** and **I10** would be a very good drug candidate suitable for further optimization. The correlation between the magnitude of the fluorescence response and the inhibitor-CA affinity was further probed in silico.

Fluorescence-Array-Based Assays

In order to investigate the utility of this dye-displacement type system and its utility in high-throughput settings, we designed a fluorescence microarray by using

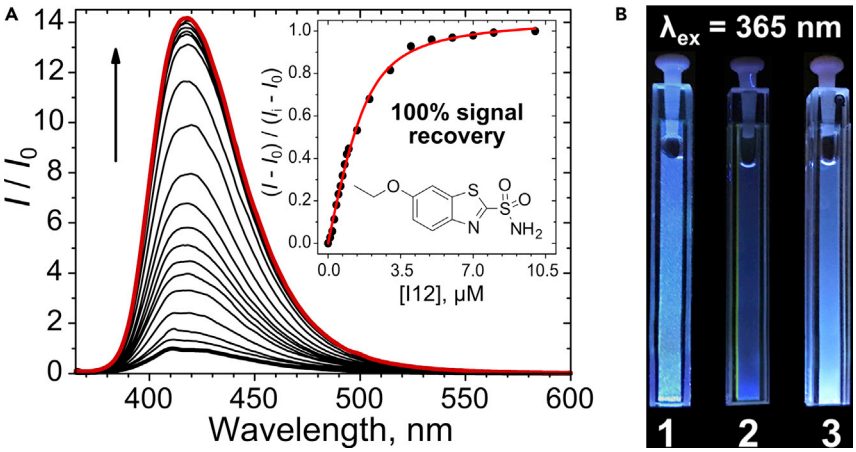


Figure 5. Competitive Fluorescence Titration of the Fluorescent Probe and bCA II with a High-Affinity Inhibitor

(A) Examples of the competitive fluorescence titration: fluorescence titration spectra of **S1** (500 nM) and bCA II (9.6 μg/mL) in aqueous HEPES solution (50 mM and pH 7.2) upon the addition of an incremental amount of **I12** with fluorescence titration isotherms (inset). λ_{EXC} = 359 nm and [**I12**] = 0–10 μM.

(B) Photograph of sensor **S1** (10 μM) in the absence (1) and presence (2) of bCA II (200 μg/mL) and after the addition of **I12** (250 μM) to the solution of **S1** and bCA II (3).

indicators **S1**, **S3**, and **S5**, which provided the best response in competitive experiments (see Supplemental Experimental Procedures and Figures S32–S52). We performed the statistical evaluation of the array response to the solutions of inhibitors by using linear discriminant analysis (LDA). LDA is a statistical method used to reduce a multidimensional dataset to achieve an easier interpretation.[47,48]

Qualitative Assay

The LDA analysis revealed an excellent recognition capability of the indicators, as illustrated by the 100% correct classification of all 8,640 trials by the leave-one-out procedure. Figure 7A shows the LDA results in a 3D response space defined by the first three canonical factors (F1–F3). Here, the indicator array recognized the inhibitors **I1**–**I14** and sorted them into three subgroups according to their structural features: aliphatic, aromatic inhibitors, and high-affinity inhibitors (commercially available drugs). This result is very important because it shows that the observed responses correlate with the structure of the inhibitors. This suggests not only that such an analysis can be used to screen ligands for potential drug development but also that the present assay can be an important tool for investigating the structure-function relationships between ligands and enzymes.

Quantitative or Semi-quantitative Assay

The positive outcome of the qualitative analysis suggested that a semi-quantitative assay could also be successful. To test this hypothesis, we set up a semi-quantitative assay by using the same set of variables to identify varying concentrations of **I5**, **I9**, **I10**, **I11**, and **I13** (Figure 7B). All five inhibitors showed a smooth isotherm-like trend, suggesting direct correlation between the response magnitude and concentration. Figures 7C and 7D show the semi-quantitative analysis utilizing F1 largely defined by the fluorescence response and concentration-dependent normalization, which highlights the difference in affinity among different inhibitors. As expected, the most efficient inhibitor, **I13** ($K_I = 8.4 \times 10^{10}\ M^{-1}$), elicits the largest magnitude in the fluorescence response from enzyme-indicator assemblies; on the other extreme, the low response of **I9** ($K_I = 2.5 \times 10^{6}\ M^{-1}$) reflects a lower affinity than that of the remaining

Table 2. Measured and Calculated Binding Affinities K_I for Inhibitors I3–I14 to Bovine Carbonic Anhydrase Isozyme II in Competitive Fluorescence Titrations

Indicator	Binding Affinity K_I (M^{-1})[a]	
	Experiment	Docking[b]
I1	NR	2.2×10^2
I2	NR	1.4×10^3
I3	1.03×10^6	6.9×10^4
I4	1.96×10^4	9.7×10^4
I5	2.91×10^6	1.4×10^5
I6	9.21×10^5	2.3×10^5
I7	3.08×10^6	1.1×10^5
I8	3.48×10^7	2.8×10^6
I9	8.30×10^4	5.5×10^3
I10	1.00×10^9	6.9×10^4
I11	9.79×10^8	8.2×10^4
I12	2.37×10^{10}	4.9×10^4
I13	1.10×10^{10}	3.0×10^4
I14	2.47×10^6	1.9×10^5
I15	5.49×10^6	1.9×10^5

[a]Indicator **S1** (500 nM) was used. Experiments were performed in aqueous HEPES buffer (50 mM and pH 7.2) at ambient temperature. The fitting errors were generally lower than 20%.
[b]Ligand docking calculations using AutoDock Vina.

inhibitors in the array. This is encouraging because it suggests that the binding affinity of the inhibitors to CA II could be evaluated just on the basis of the magnitude of their fluorescence responses reflected by the canonical factors of LDA. The results of the semi-quantitative analysis also suggest that the array should allow for a rigorous quantitative treatment. For the quantitative analysis of inhibitors **I5**, **I9**, **I10**, **I11**, and **I13**, we used a support vector machine (SVM) linear regression method, which is suitable for modeling complex responses and the nonlinear behavior of the data.[49] The SVM-based linear regression was successful and allowed for simultaneous prediction of multiple inhibitor concentrations. Here, we used eight inhibitor concentrations to model the behavior of the data and two inhibitor concentrations as a validation dataset for the model. The plots of predicted versus real concentrations for the inhibitors attest to the predictive power of the model (see Supplemental Information). Moreover, we were able to determine the limit of detection (LOD)[48] for several inhibitors: *tert*-butylbenzene sulfonamide, **I5** (LOD = 4.2 μM = 890 ppb), 2-thiophene sulfonamide, **I9** (LOD = 19.2 μM = 3 ppm), acetazolamide, **I10** (LOD = 2.1 μM = 470 ppb), methazolamide, **I11** (LOD = 2.8 μM = 660 ppb), and brinzolamide, **I13** (LOD = 14 nM = 6 ppb). Importantly, the LOD values obtained were found to be well below the usual therapeutic concentrations for these therapeutically relevant analytes.[50–52]

Molecular Modeling

Molecular modeling and docking computational analysis are currently standard tools used to narrow down large libraries of compounds into a smaller subset for experimental testing. To compare the present method with docking computations, we performed the docking analysis for inhibitors **I1**–**I14** and indicators **S1**–**S5** with hCA II. The experimental binding energies reported in Table 2 provide an excellent test set to validate the results of docking. For the docking calculations, we used

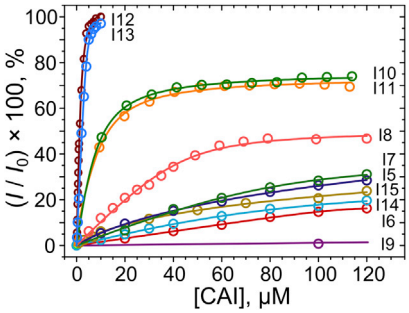


Figure 6. Competitive Fluorescence Titration Isotherms for Selected CA Inhibitors

Fluorescence titration isotherms of the competitive assay for inhibitors **I5**–**I15** as obtained from titration data with bovine carbonic anhydrase isozyme II (9.6 μg/mL) and **S1** (500 nM) in HEPES buffer (50 mM and pH 7.2).

AutoDock4$_{Zn}$[45] and AutoDock Vina[46] (details are provided in the Supplemental Information). In brief, atomic charges for the ligands were derived by restrained electrostatic potential (RESP) fitting from quantum-mechanical calculations.[53] Following the cross-docking analysis by Tuccinardi et al.,[54] we used hCA II from PDB: 1OKN as the receptor for docking. Computed docking geometries are in excellent agreement with available crystal structures (see Figure S56). However, although AutoDock4$_{Zn}$ is able to consistently predict good binding geometries because of its improved force field for coordination with zinc,[45] it underestimates the binding affinity of the ligand to the protein in comparison with experimental binding affinities reported in Table 2. Therefore, we repeated the docking with AutoDock Vina, which uses a better and faster scoring function and therefore allows for incorporation of a larger number of flexible torsions than with AutoDock4$_{Zn}$. Using Vina, we were able to include some flexible protein residues in the binding site as well. Vina produced slightly higher binding affinities than AutoDock4$_{Zn}$. Thus, these are the values we report in Tables 1 and 2 for **S1**–**S5** and **I1**–**I14**, respectively. In most cases, binding affinities computed with AutoDock Vina are still significantly smaller than experimental and literature values. Nevertheless, we find that the trends of the docking computations correlate with the experimental binding affinities, although this correlation is not strong. For instance, the calculations predict a low binding affinity for **I1** and **I2** and that **S1**–**S5** bind within the protein. However, the docking is significantly less sensitive to structural differences in ligands and is therefore not able to distinguish between ligands or inhibitors of similar affinity. Indeed, whereas experimental binding affinities cover a range of over 7 orders of magnitude, the computed ones range over 4 orders of magnitude. The reason for this discrepancy most likely stems from approximations made in the docking models. More quantitative calculations would require models that can more accurately describe all important binding site interactions between the ligand and enzyme, such as hybrid quantum mechanical/molecular mechanical (QM/MM).[55] However, constructing such models is time consuming and therefore not suitable for high-throughput screening required in the field of drug discovery and structure optimization. This underscores the importance of our approach. Our results indicate that docking tools are useful for recognizing potential inhibitors (e.g., from a large ligand pool) and classifying them as high- or low-affinity inhibitors. However, the usefulness of such simple docking models is limited when it comes to distinguishing between inhibitors that have similar binding affinities (within a few orders of magnitude), as also indicated by other docking studies on hCA II.[54] Therefore, there is a demand for the development of fast, efficient, and accurate experimental techniques complementary to docking models to screen libraries of inhibitors in a high-throughput fashion. The high-throughput dye-displacement assay tool presented here exceeds the capability of the docking calculations, which are mostly qualitative and high-cost catalytic experiments.

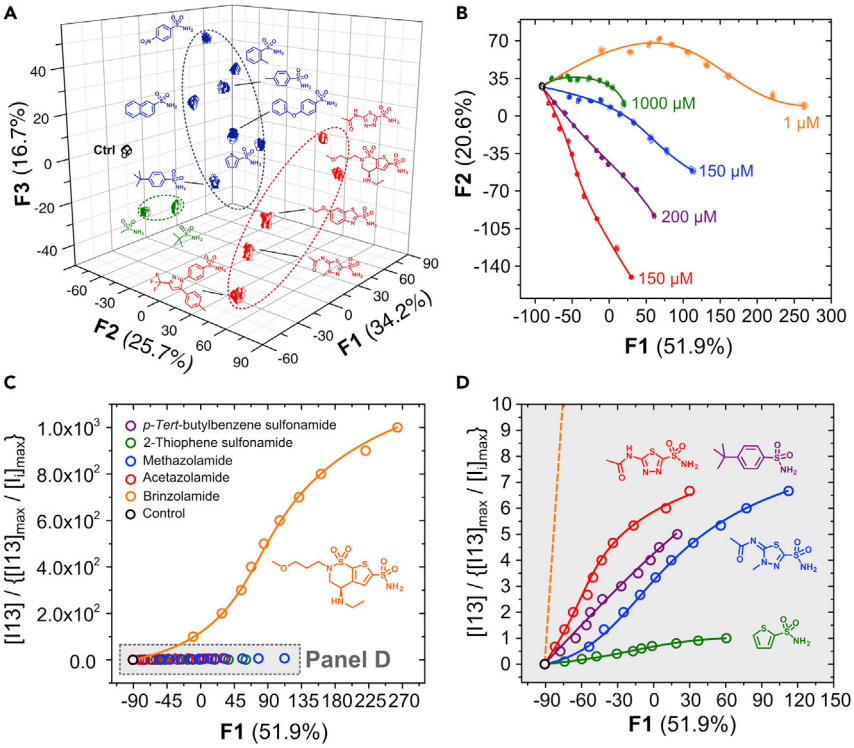


Figure 7. Results of Qualitative and Semi-quantitative Assays of CA Inhibitors

(A) Graphical output of the qualitative LDA for a competitive assay of hCA II (5 µg/mL) with inhibitors **I1**–**I14** ([hCA II]/[inhibitor] = 1: 100) and indicators **S1**, **S3**, and **S5** (500 nM).

(B) Results of the semi-quantitative LDA for a competitive assay of bCA II (5 µg/mL) with inhibitors **I5** (purple), **I9** (green), **I10** (red), **I11** (blue), and **I13** (orange). The LDA recognition capability is 100% for 50 data points with 20 repetitions in each cluster and a control with 100 repetitions within the cluster. The response space is defined by the first two factors (F1 and F2) of LDA; the 2D plot comprises 72.5% of total variance.

(C and D) Results of the semi-quantitative LDA for a competitive assay of bCA II (5 µg/mL) with inhibitors **I5**, **I9**, **I10**, **I11**, and **I13**. The response space is defined by the first factor (F1) of LDA according to concentration-dependent normalization (y axis).

Conclusions

We have developed a simple yet effective dye-displacement assay to evaluate the efficiency of inhibitors for carbonic anhydrase enzymes that bind sulfonamide inhibitors. The fluorescence-based displacement study revealed that the indicators used here display on-off behavior such that the fluorescence is largely quenched in the presence of CA but is recovered in the presence of an enzyme inhibitor. The indicators described here enable an array-based displacement assay for various potential and standard CA inhibitors. This assay allows qualitative study of the inhibitors and evaluation of their structure for application as CA inhibitors. The present qualitative study enabled the selection of potential inhibitors and evaluated their CA-binding affinities in a quantitative manner. Finally, the fluorescence assay was compared with a standard tool of drug discovery, computer-generated docking models. The docking results validated the results of the displacement approach and confirmed that these tools are useful for recognizing potential inhibitors and classifying them as high- or low-affinity inhibitors. However, the utility of the standard docking models is limited when it comes to distinguishing between inhibitors that have similar binding affinities, which is the strong point of the displacement assay. The high-throughput dye-displacement assay tool presented in the present work

complements the docking analysis tools, which are mostly qualitative, by providing a valuable quantitative insight.

EXPERIMENTAL PROCEDURES

The experimental procedures and details on molecular modeling are included in the Supplemental Information.

ACCESSION NUMBERS

S3 crystallographic data have been deposited in the Cambridge Crystallographic Data Centre under accession number CCDC: 1526920.

SUPPLEMENTAL INFORMATION

Supplemental Information includes Supplemental Experimental Procedures, 56 figures, 19 tables, 6 schemes, and 11 additional NMR spectral data files and can be found with this article online at http://dx.doi.org/10.1016/j.chempr.2017.01.011.

AUTHOR CONTRIBUTIONS

P.K. conceived the synthesis of the sensors and the spectroscopic experiments and performed these experiments. E.G.S. conceived and performed the high-throughput array experiments. M.G.C. developed the competitive binding-constant model. S.G. conceived and performed the computational and docking work. T.M. helped to conceive the project. P.A. conceived the project and wrote the manuscript.

ACKNOWLEDGMENTS

Funding from Bowling Green State University and the National Science Foundation (CHE-0750303 and DMR-1006761) are gratefully acknowledged. We would like to acknowledged Dr. V.M. Lynch of the University of Texas at Austin for SXRD data collection and interpretation.

Received: October 15, 2016
Revised: November 9, 2016
Accepted: January 19, 2017
Published: February 9, 2017

REFERENCES AND NOTES

1. Krishnamurthy, V.M., Kaufman, G.K., Urbach, A.R., Gitlin, I., Gudiksen, K.L., Weibel, D.B., and Whitesides, G.M. (2008). Carbonic anhydrase as a model for biophysical and physical-organic studies of proteins and protein–ligand binding. Chem. Rev. *108*, 946–1051.

2. Supuran, C.T. (2008a). Carbonic anhydrases: novel therapeutic applications for inhibitors and activators. Nat. Rev. Drug Discov. *7*, 168–181.

3. Imtaiyaz Hassan, M., Shajee, B., Waheed, A., Ahmad, F., and Sly, W.S. (2013). Structure, function and applications of carbonic anhydrase isozymes. Bioorg. Med. Chem. *21*, 1570–1582.

4. Lindskog, S., and Nyman, P.O. (1964). Metal-binding properties of human erythrocyte carbonic anhydrases. Biochim. Biophys. Acta *85*, 462–474.

5. Supuran, C.T. (2008b). Carbonic anhydrases - an overview. Curr. Pharm. Des. *14*, 603–614.

6. Esbaugh, A.J., and Tufts, B.L. (2006). The structure and function of carbonic anhydrase isozymes in the respiratory system of vertebrates. Respir. Physiol. Neurobiol. *154*, 185–198.

7. Lindskog, S. (1997). Structure and mechanism of carbonic anhydrase. Pharmacol. Ther. *74*, 1–20.

8. Silverman, D.N., and Lindskog, S. (1988). The catalytic mechanism of carbonic anhydrase: implications of a rate-limiting protolysis of water. Acc. Chem. Res. *21*, 30–36.

9. Berg, J.M., Tymoczko, J.L., Stryer, L., and Stryer, L. (2002). Biochemistry (W.H. Freeman).

10. Supuran, C.T. (2008c). Diuretics: from classical carbonic anhydrase inhibitors to novel applications of the sulfonamides. Curr. Pharm. Des. *14*, 641–648.

11. Fishman, R.A. (1975). Brain edema. N. Engl. J. Med. *293*, 706–711.

12. Mincione, F., Scozzafava, A., and Supuran, C.T. (2008). The development of topically acting carbonic anhydrase inhibitors as antiglaucoma agents. Curr. Pharm. Des. *14*, 649–654.

13. Liao, S.-Y., Ivanov, S., Ivanova, A., Ghosh, S., Cote, M.A., Keefe, K., Coca-Prados, M., Stanbridge, E.J., and Lerman, M.I. (2003). Expression of cell surface transmembrane carbonic anhydrase genes CA9 and CA12 in the human eye: overexpression of CA12 (CAXII) in glaucoma. J. Med. Genet. *40*, 257–261.

14. De Simone, G., and Supuran, C.T. (2007). Antiobesity carbonic anhydrase inhibitors. Curr. Top. Med. Chem. *7*, 879–884.

15. Supuran, C.T., Fiore, A.D., and Simone, G.D. (2008). Carbonic anhydrase inhibitors as emerging drugs for the treatment of obesity. Expert Opin. Emerg. Drugs *13*, 383–392.

16. Thiry, A., Dogné, J.-M., Masereel, B., and Supuran, C.T. (2006). Targeting tumor-associated carbonic anhydrase IX in cancer therapy. Trends Pharmacol. Sci. *27*, 566–573.

17. Koukourakis, M.I., Giatromanolaki, A., Sivridis, E., Simopoulos, K., Pastorek, J., Wykoff, C.C., Gatter, K.C., and Harris, A.L. (2001). Hypoxia-regulated carbonic anhydrase-9 (CA9) relates to poor vascularization and resistance of squamous cell head and neck cancer to chemoradiotherapy. Clin. Cancer Res. *7*, 3399–3403.

18. Dodgson, S.J., Shank, R.P., and Maryanoff, B.E. (2000). Topiramate as an inhibitor of carbonic anhydrase isoenzymes. Epilepsia *41* (*Suppl 1*), S35–S39.

19. De Simone, G., Scozzafava, A., and Supuran, C.T. (2009). Which carbonic anhydrases are targeted by the antiepileptic sulfonamides and sulfamates? Chem. Biol. Drug Des. *74*, 317–321.

20. Swenson, E.R., and Teppema, L.J. (2006). Prevention of acute mountain sickness by acetazolamide: as yet an unfinished story. J. Appl. Physiol. *102*, 1305–1307.

21. Basnyat, B., Gertsch, J.H., Johnson, E.W., Castro-Marin, F., Inoue, Y., and Yeh, C. (2003). Efficacy of low-dose acetazolamide (125 mg BID) for the prophylaxis of acute mountain sickness: a prospective, double-blind, randomized, placebo-controlled trial. High Alt. Med. Biol. *4*, 45–52.

22. Riihonen, R., Supuran, C.T., Parkkila, S., Pastorekova, S., Väänänen, H.K., and Laitala-Leinonen, T. (2007). Membrane-bound carbonic anhydrases in osteoclasts. Bone *40*, 1021–1031.

23. Kivelä, J., Parkkila, S., Parkkila, A.K., and Rajaniemi, H. (1999). A low concentration of carbonic anhydrase isoenzyme VI in whole saliva is associated with caries prevalence. Caries Res. *33*, 178–184.

24. Supuran, C., and Scozzafava, A. (2001). Carbonic anhydrase inhibitors. Curr. Med. Chem. *1*, 61–97.

25. Alterio, V., Di Fiore, A., D'Ambrosio, K., Supuran, C.T., and De Simone, G. (2012). Multiple binding modes of inhibitors to carbonic anhydrases: how to design specific drugs targeting 15 different isoforms? Chem. Rev. *112*, 4421–4468.

26. Keilin, D., and Mann, T. (1940). Carbonic anhydrase. Purification and nature of the enzyme. Biochem. J. *34*, 1163–1176.

27. Supuran, C.T., Scozzafava, A., and Conway, J. (2004). Carbonic Anhydrase: Its Inhibitors and Activators (CRC Press).

28. Supuran, C.T., Scozzafava, A., and Casini, A. (2003). Carbonic anhydrase inhibitors. Med. Res. Rev. *23*, 146–189.

29. Grüneberg, S., Stubbs, M.T., and Klebe, G. (2002). Successful virtual screening for novel inhibitors of human carbonic anhydrase: strategy and experimental confirmation. J. Med. Chem. *45*, 3588–3602.

30. Shoichet, B.K., McGovern, S.L., Wei, B., and Irwin, J.J. (2002). Lead discovery using molecular docking. Curr. Opin. Chem. Biol. *6*, 439–446.

31. Esposito, E.X., Baran, K., Kelly, K., and Madura, J.D. (2000). Docking of sulfonamides to carbonic anhydrase II and IV. J. Mol. Graph. Model. *18*, 283–289, 307–308.

32. McIntosh, J.E.A. (1968). Assay of carbonic anhydrase by titration at constant pH. Biochem. J. *109*, 203–207.

33. Khalifah, R.G. (1971). The carbon dioxide hydration activity of carbonic anhydrase. I. Stop-flow kinetic studies on the native human isoenzymes B and C. J. Biol. Chem. *246*, 2561–2573.

34. Cecchi, A., Hulikova, A., Pastorek, J., Pastoreková, S., Scozzafava, A., Winum, J.-Y., Montero, J.-L., and Supuran, C.T. (2005). Carbonic anhydrase inhibitors. design of fluorescent sulfonamides as probes of tumor-associated carbonic anhydrase IX that inhibit isozyme IX-mediated acidification of hypoxic tumors. J. Med. Chem. *48*, 4834–4841.

35. Carta, F., Ferraroni, M., Scozzafava, A., and Supuran, C.T. (2016). Fluorescent sulfonamide carbonic anhydrase inhibitors incorporating 1,2,3-triazole moieties: kinetic and X-ray crystallographic studies. Bioorg. Med. Chem. *24*, 104–112.

36. Nguyen, B.T., and Anslyn, E.V. (2006). Indicator–displacement assays. Coord. Chem. Rev. *250*, 3118–3127.

37. Mizusawa, K., Ishida, Y., Takaoka, Y., Miyagawa, M., Tsukiji, S., and Hamachi, I. (2010). Disassembly-driven turn-on fluorescent nanoprobes for selective protein detection. J. Am. Chem. Soc. *132*, 7291–7293.

38. Tsukiji, S., Wang, H., Miyagawa, M., Tamura, T., Takaoka, Y., and Hamachi, I. (2009). Quenched ligand-directed tosylate reagents for one-step construction of turn-on fluorescent biosensors. J. Am. Chem. Soc. *131*, 9046–9054.

39. Wagner, B.D. (2009). The use of coumarins as environmentally-sensitive fluorescent probes of heterogeneous inclusion systems. Molecules *14*, 210–237.

40. Zhuang, Y.-D., Chiang, P.-Y., Wang, C.-W., and Tan, K.-T. (2013). Environment-sensitive fluorescent turn-on probes targeting hydrophobic ligand-binding domains for selective protein detection. Angew. Chem. Int. Ed. Engl. *52*, 8124–8128.

41. Wang, S.C., and Zamble, D.B. (2006). Fluorescence analysis of sulfonamide binding to carbonic anhydrase. Biochem. Mol. Biol. Educ. *34*, 364–368.

42. Teruya, K., Tonissen, K.F., and Poulsen, S.-A. (2016). Recent developments of small molecule chemical probes for fluorescence-based detection of human carbonic anhydrase II and IX. Med. Chem. Commun. *7*, 2045–2062.

43. Saito, R., Sato, T., Ikai, A., and Tanaka, N. (2004). Structure of bovine carbonic anhydrase II at 1.95 Å resolution. Acta Crystallogr. D Biol. Crystallogr. *60*, 792–795.

44. He, X.M., and Carter, D.C. (1992). Atomic structure and chemistry of human serum albumin. Nature *358*, 209–215.

45. Santos-Martins, D., Forli, S., Ramos, M.J., and Olson, A.J. (2014). AutoDock4$_{Zn}$: an improved autodock force field for small-molecule docking to zinc metalloproteins. J. Chem. Inf. Model. *54*, 2371–2379.

46. Trott, O., and Olson, A.J. (2009). AutoDock Vina: improving the speed and accuracy of docking with a new scoring function, efficient optimization, and multithreading. J. Comput. Chem. *31*, 455–461.

47. Brereton, R.G. (2007). Applied Chemometrics for Scientists (John Wiley).

48. Miller, J.N., and Miller, J.C. (2010). Statistics and Chemometrics for Analytical Chemistry (Prentice Hall).

49. Hamel, L. (2009). Knowledge Discovery with Support Vector Machines (John Wiley).

50. McCannel, C.A., Heinrich, S.R., and Brubaker, R.F. (1992). Acetazolamide but not timolol lowers aqueous humor flow in sleeping humans. Graefes Arch. Clin. Exp. Ophthalmol. *230*, 518–520.

51. Maren, T.H., Haywood, J.R., Chapman, S.K., and Zimmerman, T.J. (1977). The pharmacology of methazolamide in relation to the treatment of glaucoma. Invest. Ophthalmol. Vis. Sci. *16*, 730–742.

52. DeSantis, L. (2000). Preclinical overview of brinzolamide1. Surv. Ophthalmol. *44*, S119–S129.

53. Bayly, C.I., Cieplak, P., Cornell, W., and Kollman, P.A. (1993). A well-behaved electrostatic potential based method using charge restraints for deriving atomic charges: the RESP model. J. Phys. Chem. *97*, 10269–10280.

54. Tuccinardi, T., Nuti, E., Ortore, G., Supuran, C.T., Rossello, A., and Martinelli, A. (2007). Analysis of human carbonic anhydrase ii: docking reliability and receptor-based 3D-QSAR study. J. Chem. Inf. Model. *47*, 515–525.

55. Sahu, C., Sen, K., Pakhira, S., Mondal, B., and Das, A.K. (2013). Binding affinity of substituted ureido-benzenesulfonamide ligands to the carbonic anhydrase receptor: a theoretical study of enzyme inhibition. J. Comput. Chem. *34*, 1907–1916.